

## Photoelectron spectroscopy for the study of reactions on surfaces

This article has been downloaded from IOPscience. Please scroll down to see the full text article.

2001 J. Phys.: Condens. Matter 13 11293

(<http://iopscience.iop.org/0953-8984/13/49/312>)

View [the table of contents for this issue](#), or go to the [journal homepage](#) for more

### Download details:

IP Address: 171.66.16.238

The article was downloaded on 17/05/2010 at 04:39

Please note that [terms and conditions apply](#).

# Photoelectron spectroscopy for the study of reactions on surfaces

**G Paolucci**

Sincrotrone Trieste S.C.p.A., S.S. 14 Km 163.5, in Area Science Park, 34012 Trieste, Italy

E-mail: [giorgio.paolucci@elettra.trieste.it](mailto:giorgio.paolucci@elettra.trieste.it)

Received 26 September 2001

Published 10 December 2001

Online at [stacks.iop.org/JPhysCM/13/11293](http://stacks.iop.org/JPhysCM/13/11293)

## Abstract

The combination of new-undulator-based synchrotron radiation sources with state-of-the-art electron detection systems has allowed major improvements in the study of gas–surface interactions. In particular, the high photon flux, high energy resolution and high data acquisition speed have rendered it possible to use x-ray photoelectron spectroscopy (XPS) to follow the kinetics of gas–surface interactions while they occur. In this paper, some examples of the use of the *fast-XPS* technique are presented.

(Some figures in this article are in colour only in the electronic version)

## 1. Introduction

Since the early days of photoelectron spectroscopy, it has been suggested that its surface sensitivity combined with its ability to distinguish between different chemical species could be used to study chemical reactions on solid surfaces while they occur. However, for many years the acquisition time needed for measuring an x-ray photoelectron spectroscopy (XPS) spectrum with sufficient energy resolution and good signal-to-noise ratio has been too long for following the evolution of the chemical species present on the surface in the ongoing reaction. For this reason the use of the XPS technique was restricted to cases in which it was possible to freeze the reaction under study [1]. This has been useful in a number of cases for characterizing the properties of chemisorption systems, but did not allow the study of the kinetics of gas–surface interactions. This is now possible due to the development of third-generation-undulator-based synchrotron radiation sources, combined with that of new electron energy analysers and electron detection systems which allow the proper combination of energy resolution and speed of data acquisition necessary to follow a surface reaction. In this paper the achievements obtained at the SuperESCA beamline of Elettra, the Italian third-generation synchrotron radiation facility in Trieste, are presented. The paper is organized as follows: in section 2 the factors motivating the use of photoelectron spectroscopy for the study of surface reactions are given; section 3 gives a description of the experimental apparatus and

of the electron detection system; in section 4 an overview of fast-XPS studies performed on the SuperESCA beamline is presented.

## 2. XPS and surface chemistry

In order to understand a chemical process that takes place on a surface it is necessary to know, first of all, what the chemical species that are present on the surface are. Moreover, not only is the chemical identity important, but so also are the following: what the adsorption site of an atom or molecule is; whether the adsorption of a molecule is dissociative or not; what the structural changes involved in the surface process are; and what the amount of a certain chemical species is in certain experimental conditions. There are a number of surface science techniques which can be combined in order to conduct these studies such as low-energy electron diffraction (LEED), thermal desorption spectroscopy (TDS), high-resolution electron energy-loss spectroscopy (HREELS), infrared reflection absorption spectroscopy (IRAS), scanning tunnelling microscopy (STM). XPS is also a powerful method, as the position of an XPS peak depends on the chemical species and on the chemical environment of the emitting atom. Moreover, the intensity of an XPS peak is directly related to the coverage of the species on the surface. However, in order to study the time evolution of the adsorbed species, only TDS and vibrational spectroscopy (i.e. IRAS and HREELS) could be used until a few years ago. These methods have however limitations in their applicability:

- (i) TDS measures the *desorbed* species, so information on the evolution of the *adsorbed* species can only be indirectly deduced;
- (ii) the intensities of the features in vibrational spectroscopies are not directly proportional to the coverage of the corresponding species and therefore the determination of the population of the species can be extremely difficult.

XPS does not suffer from these limitations, but, as mentioned before, until the development of third-generation synchrotron radiation sources, its main limitation was the data acquisition speed. With the new sources it is now possible to have beamlines delivering a photon flux as high as  $10^{12}$  photons  $s^{-1}$  with a resolving power  $E/\Delta E$  of the order of  $10^4$  [2]. For this reason it is now possible to follow surface chemical reactions as they occur.

## 3. Experimental procedure

The SuperESCA beamline was described in [2]. The source is an undulator with a 5.6 cm period and the beamline is based on a modification of Petersen's SX700 [3] to match the high undulator brilliance [4]. In normal operation, the usable photon energy ranges from 80 to 1200 eV. The experiments described in sections 4.1–4.4 were performed with a modified VSW CLASS 150 electron energy analyser, equipped with a 16-channel detector. In the other experiments, the experimental station was equipped with a double-pass 150 mm hemispherical electron energy analyser [5]. This design allows performances comparable to that of a 300 mm single-pass hemispherical analyser. The analyser mounts a novel detector with 96 discrete parallel channels [6]. The detector allows one to measure a 96-point spectrum in a single shot, provided of course that the signal-to-noise ratio is good enough. Other detection schemes allow parallel detection, but the scheme chosen at the SuperESCA has at least the following advantages:

- (i) The frequency response of the analogue section of the electronics goes up to 25 MHz per channel, which is much higher than the actual count rate that a microchannel plate can actually stand.

- (ii) The detector response is linear as long as the electron multiplier is linear.
- (iii) Because the actual count rate is measured, the noise is given directly by Poisson statistics.
- (iv) The embedded computer architecture allows very fast data acquisition, the minimum integration time being 50 ns.

Such a detector can produce very high data flow. For this reason, the detector is equipped with an embedded computer [6] which takes care of efficiently transferring the data to the host computer. The 96-channel data are transferred to the host computer in about 1 ms. For shorter data acquisition times, the system has the possibility of storing the data in its memory before transferring them to the host computer. In this way very short measurement times are possible.

Recently a supersonic molecular beam system has been added to the experimental chamber [7]. This instrument allows one to perform experiments in which the state of the incoming molecules can be controlled: it is indeed possible to vary both modulus and direction of the molecule velocity and also to control accurately the exposure. The first measurements with this instruments are described in section 4.6.

#### 4. Selected systems

The use of fast XPS has allowed study of a number of surface adsorption systems. The method is particularly useful as it allows one to detect chemisorption states which could not be identified by 'static' measurements. In this section some of the results so far obtained are displayed.

##### 4.1. Desorption of CO from Rh(110)

One of the first applications of fast XPS was the extension of TDS [8]. In TDS one usually measures the desorption rate of adsorbed species from surfaces while a temperature ramp is applied to the sample. The technique is not very demanding from the instrumental point of view as it only needs a mass spectrometer and accurate sample temperature control. However, the technique only measures *desorbed* species while processes occurring on the surface such as bond breaking or recombination can only be indirectly inferred. The observation of such processes can be achieved by vibrational spectroscopies, but they suffer from two severe limitations:

- (i) atomic species are not clearly measured because the atom–substrate vibrational frequency is usually very low;
- (ii) the correlation between intensity and coverage of a given species is not always linear.

For this reason we investigated the possibility of using XPS as a direct probe of surface chemical modifications in real time. Figure 1 shows a series of O 1s spectra measured from CO-predosed Rh(110) while a temperature ramp of  $0.3 \text{ K s}^{-1}$  was applied to the sample. The surface had been saturated with CO at a sample temperature of  $\approx 200 \text{ K}$ , giving rise to a sharp  $(2 \times 1) p2mg$  LEED pattern. Figure 1 shows immediately the processes occurring on the surface: the overall reduction of the O 1s signal is a clear indication of the desorption which is taking place, while one can also see that the XPS peak shifts from 530.8 to 531.9 eV. This latter behaviour is an indication that CO is changing its bonding on the surface and, from previous studies [9], it is known that the two binding energies correspond to bridge and on-top-bonded CO molecules, respectively. Standard evaluation of the individual XPS [10, 11] spectra allows one to decompose each one into the bridge and on-top components leading to the behaviour shown in figure 2, which highlights the fact that migration from bridge to on-top sites occurs in the range from  $\approx 350$  to  $\approx 400 \text{ K}$ .

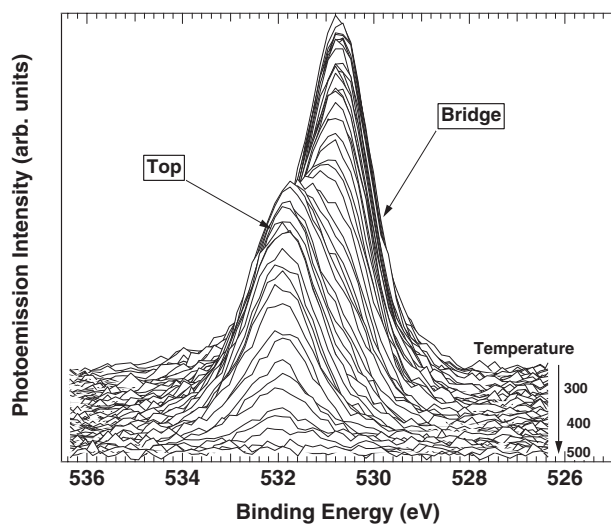


**Figure 1.** O 1s spectra from a CO-precovered Rh(110) surface measured while a linear temperature ramp of  $0.3 \text{ K s}^{-1}$  is applied to the sample [8].

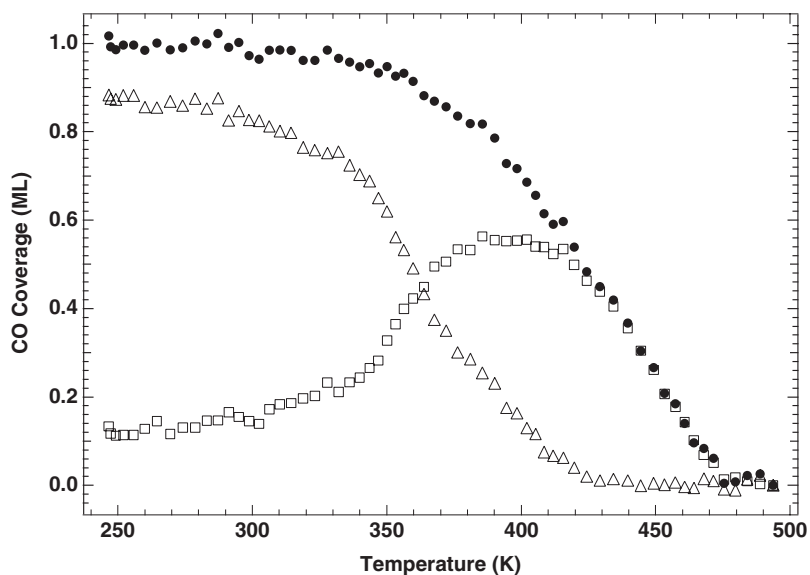


**Figure 2.** Total CO coverage (●) and coverage of the two CO species (bridge: △; top: □) as determined from the data in figure 1.

#### 4.2. Dissociative oxygen adsorption on Rh(110)

Oxygen adsorption on Rh(110) at sample temperatures of about 570 K induces  $1 \times n$  reconstructions of the substrate [12] which, on the other hand, modify the reactivity of the surface. This means that the reactivity towards oxygen is modified by the presence of oxygen itself. By fast XPS, looking at the O 1s core level, we measured the uptake of oxygen in the non-reconstructing (at 270 K) and reconstructing (at 570 K) conditions. The behaviour of the various components of the XPS spectra is shown in figure 3.

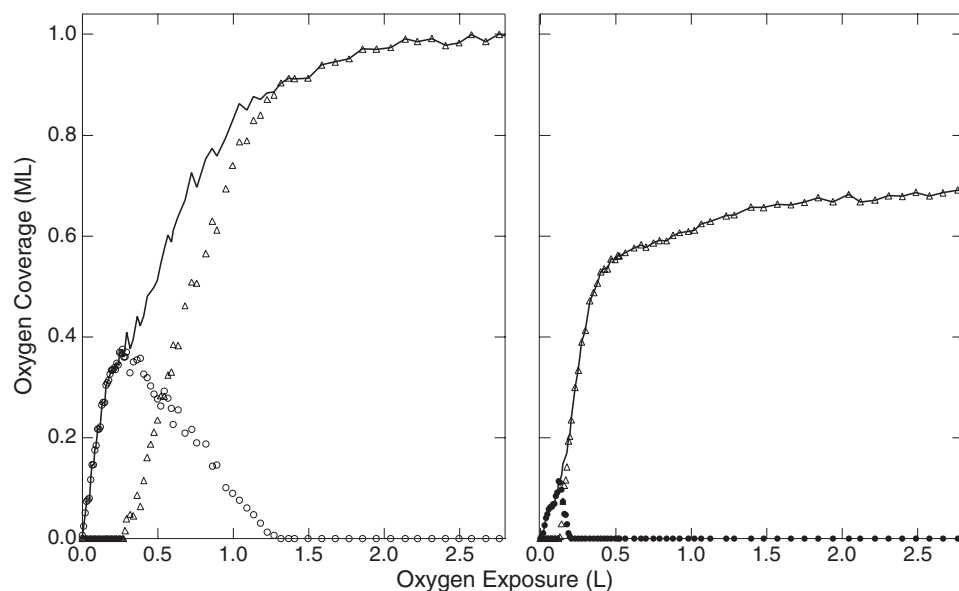


**Figure 3.** Oxygen uptake plots [13]. The left panel corresponds to oxygen dosing at a sample temperature of 270 K, while the right panel shows a plot of the uptake curves measured at 570 K. The continuous curves (—) show the total oxygen coverage, the triangles ( $\Delta$ ) refer to oxygen adsorbed in threefold sites (whose O 1s binding energy is  $530.25 \pm 0.05$  eV) and the open circles ( $\circ$ ) and the filled circles ( $\bullet$ ) indicate the adsorption kinetics in long bridge sites (whose O 1s binding energy is  $\sim 529.6$  eV).

From previous studies [12] we knew of the correspondence between a given O 1s binding energy and the adsorption site. So the O 1s binding energy was used as a fingerprint of the adatom adsorption geometry and the O 1s intensity as a measure of the oxygen coverage. The short data collection time allowed us to follow the conversion between different oxygen bonding configurations and to correlate it with the observed coverage and structural changes. In figure 3 the coverage of oxygen in long bridge and threefold sites, as deduced from two sets of XPS data measured at 270 and 570 K respectively, is shown. The reconstruction occurring at 570 K makes threefold sites immediately available for the adsorption, which explains the difference in behaviour of the two cases.

#### 4.3. CO titration on Rh(110)

In this experiment, we studied the interaction of CO with a  $(2 \times 1)p2mg$  oxygen layer on  $(1 \times 1)$ -Rh(110) and a  $c(2 \times 8)$  oxygen layer on  $(1 \times 4)$ -Rh(110). We combined real-time XPS with LEED and mass spectrometry. As an example, we show in figure 4 two sets of XPS spectra measured at 200 K while exposing O  $(2 \times 1)p2mg$  (left) and O  $c(2 \times 8)$  surfaces to  $5 \times 10^{-9}$  mbar of CO. The intensity of the components of the O 1s spectra reflects the changes in the oxygen and CO coverages during the reaction. The intensity decrease of the O 1s peak at binding energies  $\leq 530.3$  eV, corresponding to the adsorbed oxygen, is a measure of the CO oxidation rate. The emergence and increase of a second O 1s peak at binding energies  $\geq 531.0$  eV corresponds to the CO uptake. The changes in the CO<sub>2</sub> partial pressure during titration of the oxygen layers with CO were also monitored by a mass spectrometer. Individual O 1s spectra measured under different experimental conditions are shown in figure 5. The observed difference in reactivity of the  $(2 \times 1)p2mg$  and  $c(2 \times 8)$  layers is related to the

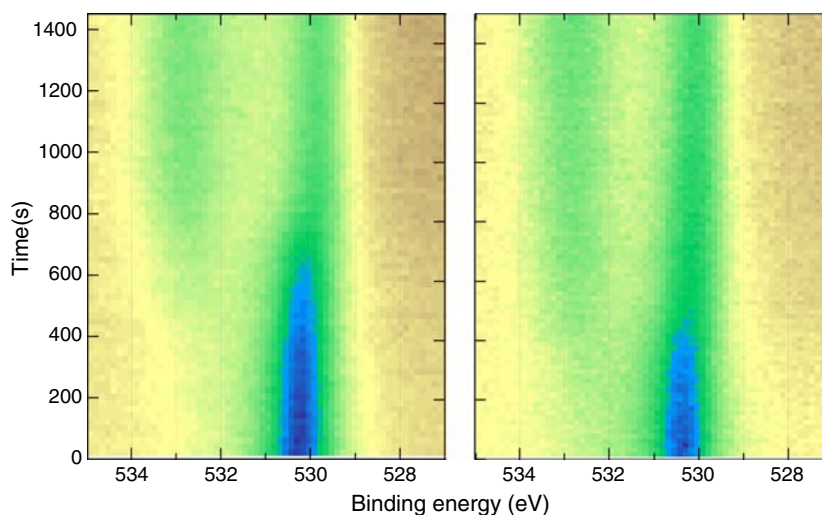


**Figure 4.** Images representing the evolution of the O 1s spectrum during CO titration at 200 K of O ( $2 \times 1$ ) $p2mg$  (left) and O  $c(2 \times 8)$  on Rh(110) (right) [14].

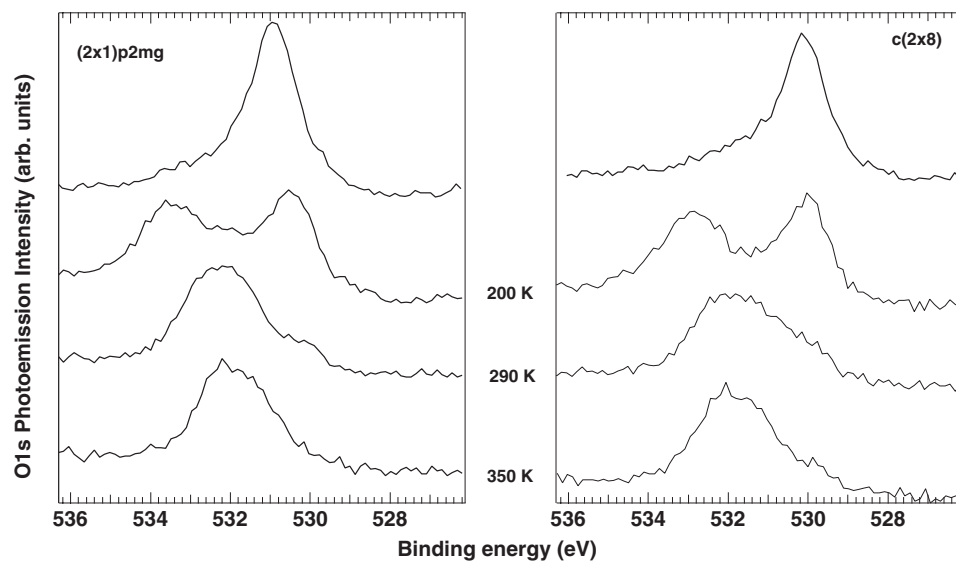


**Figure 5.** O 1s spectra measured after 20 L CO exposure during the CO titration reaction on Rh(110) on the ( $2 \times 1$ ) $p2mg$  surface (left panel) and on the  $c(2 \times 8)$  surface (right panel). The initial spectrum and the spectra measured at 200, 290 and 350 K are shown in each case [14].

structural differences of the two surfaces: the ( $1 \times 4$ ) reconstruction creates adsorption sites where oxygen is more strongly bound and less reactive. The effect of the structural changes on the reaction rate was observed during the titration reaction at 350 K.

#### 4.4. NO adsorption and dissociation on Rh(110)

The Rh(110) surface is known to induce dissociation of NO at temperatures above 200 K [15, 16]. We studied NO adsorption on Rh(110) by synchrotron radiation x-ray photoemission

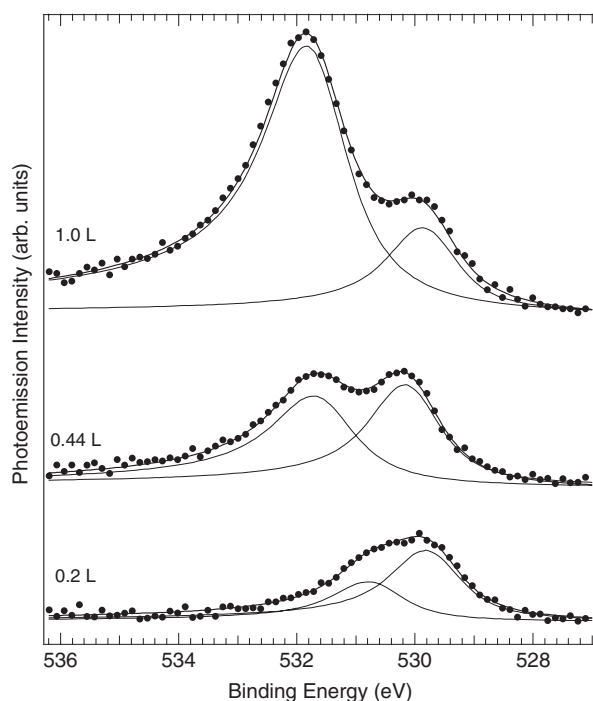


**Figure 6.** Full circles (●): O 1s spectra for three different NO doses at  $T = 270$  K. Lines: fitting components assigned to the upright and ‘lying-down’ NO and to the atomic species and the sum of the fits. The ‘lying-down’ NO component is clearly seen in the spectrum taken at 0.2 L [17]. The shift in binding energy of the lowest energy component (atomic oxygen) is interpreted as a change in the oxygen bonding, as shown in [13].

spectroscopy at temperatures in the range 210–370 K. We measured O 1s or N 1s spectra every 14 s while the surface was continuously exposed to a steady NO gas pressure. The difference in binding energies for the atomic oxygen (O 1s, 530.2 eV), atomic nitrogen (N 1s,  $\approx 397.2$  eV) and molecular upright bonded NO molecules (O 1s, 531.0 eV and N 1s, 400 eV) allowed us to distinguish these surface species and to follow the evolution of the adsorbate layer. In addition to these dominating surface species, a new species, characterized by O 1s binding energy of 530.7 eV and N 1s binding energy similar to that of the atomic nitrogen, was detected within a narrow coverage range. The occurrence of this new species is illustrated in the selection of O 1s spectra in figure 6. We tentatively assign this state to a ‘lying-down’ NO bonding configuration, detectable at the timescale of the measurements. Uptake plots, shown in figure 7, have been constructed using the integrated intensity of the O 1s components. They can be used to elucidate the effects of the reaction temperature and surface coverage and composition on the kinetics of dissociative and molecular NO adsorption on Rh(110). Of particular relevance in this case is the fact that the ‘lying down’ could not be better characterized, as all attempts to ‘freeze’ the reaction when the 530.7 eV component was seen failed, so it was impossible to perform structural measurements, such as state-selected photoelectron diffraction. This is a clear example of the strength of real-time measurements.

#### 4.5. Oxygen on $Ru(10\bar{1}0)$

In the previous examples we have shown the ability of XPS to distinguish between different adsorption sites by measuring the changes in the core levels of the adsorbates. Adsorption



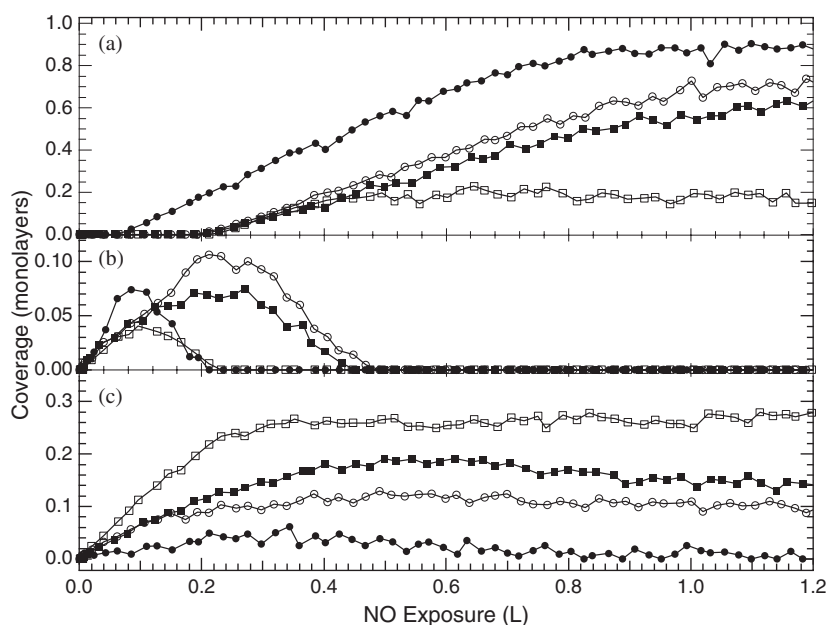


**Figure 7.** Plots of the O 1s intensity versus NO exposure for (a) upright NO, (b) 'lying-down' NO and (c) atomic oxygen. Different markers correspond to different temperatures: (●) 210 K, (○) 240 K, (■) 270 K, (□) 370 K [17].

also modifies the substrate core levels, which can therefore also be used as a fingerprint of the adsorption site [10]. The high energy resolution allows measuring with great accuracy the changes in the surface core-level shift (SCLS) induced by adsorption. Figure 8(a) shows the evolution of the Ru  $3d_{5/2}$  core level during exposure of a Ru(10 $\bar{1}$ 0) surface to O<sub>2</sub>. The spectrum is rather complex as six components (five surface components plus the bulk component) are identified. Figure 8(b) shows the evolution of the various components with O coverage. By analysing this behaviour it was possible to unambiguously assign the oxygen adsorption site as threefold hcp. The details of the interpretation of these data can be found in [18] and [19]. It is interesting to note here that for a coverage of half of a monolayer a  $c(2 \times 4)$  LEED pattern is observed which is in principle compatible with several different structures. The simple experimental observation that for this coverage the intensity of the component corresponding to the clean Ru atoms of the outermost layer (yellow) goes to zero allows one to discard all structural models in which no oxygen atom binds to the top-layer Ru atoms.

#### 4.6. Molecular beam

The latest development in the application of XPS to the study of reactions on surfaces was the combination with a supersonic molecular beam. Molecular beams are widely used in surface science (see e.g. [20]), but, as already stated, until the development of third-generation synchrotron radiation sources their use in combination with XPS was virtually impossible. The details on the experimental set-up are given elsewhere [7], and here we show an example of the strength of the combination. We have studied the reaction between oxygen and hydrogen on the Pt<sub>50</sub>Rh<sub>50</sub>(100) single-crystal surface. We followed the reaction by monitoring the Pt  $4f_{7/2}$  core level, which exhibits a pronounced surface core-level shift of 0.69 eV. Due to the 96-channel detector [6], we have been able to measure the Pt  $4f_{7/2}$  core level in snapshot mode,

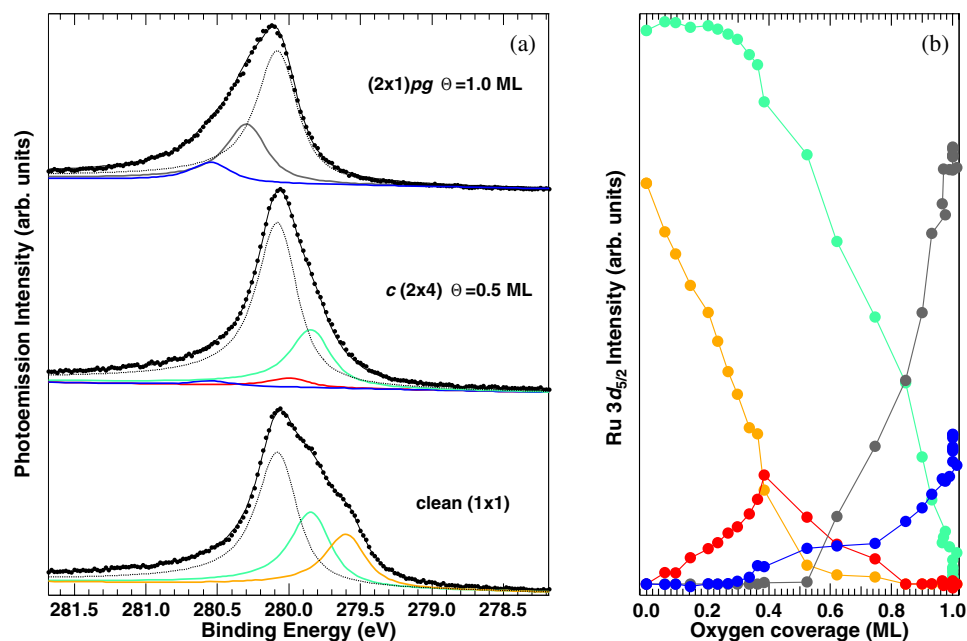


**Figure 8.** (a) Ru 3d<sub>5/2</sub> core-level spectra from Ru(10 $\bar{1}$ 0) recorded at 300 K during oxygen uptake: (bottom) clean (1 × 1); (centre) c(2 × 4); (top) (2 × 1)pg. Fits of the surface component are presented. (b) Results of the fit. The coloured curves represent: (orange) first-layer Ru, (green) second-layer Ru, (red) first-layer single-oxygen-bonded Ru, (blue) second-layer double-oxygen-bonded Ru and (grey) first-layer double-oxygen-bonded Ru [18].

i.e. without scanning the analyser voltages. Such a spectrum is shown in figure 9(a). A kinetic energy of about 100 eV ( $h\nu = 185$  eV for Pt 4f<sub>7/2</sub>) has been used in order to enhance the signal from the top-layer atoms. We have dosed with O<sub>2</sub> using the molecular beam, modulating the flux by opening and closing the shutter with different periods and duty cycles (rising constantly below 100 ms) while the sample was exposed to a continuous hydrogen flux produced by a multichannel array doser. The advantage of this approach is that the rise time of the chopped supersonic molecular beam is much lower than that of an effusion system and permits one to control in a very precise way the oxygen exposure. The evolution of the Pt surface and bulk composition due to oxygen adsorption with the surface (beam ON) and hydrogen reaction (beam OFF) is shown in figure 9(b). In our experimental conditions, oxygen does not bind to Pt atoms, but only to Rh atoms [21]. Therefore the intensity of the surface and bulk components for Pt 4f<sub>7/2</sub> reflects the population of the top and sub-surface layers respectively. The modulation of the Pt bulk component indicates that the sub-surface layers of the alloy become enriched with platinum when oxygen reacts with hydrogen to form water. Vice versa, the Pt sub-surface population decreases when oxygen adsorbs on the surface; in this case the sub-surface layers become Rh enriched. The results are in good agreement with previous experimental findings, but the advantage of this approach is that the kinetics of surface and sub-surface compositions can now be simultaneously followed in a controlled way with a time resolution of 100 ms.

## 5. Conclusions and outlook

We have shown a variety of examples of the application of fast XPS to chemisorption systems. In each case the possibility of making the measurements *while* the surface was being modified by the reaction allowed information to be obtained on the energetics and on the kinetics of

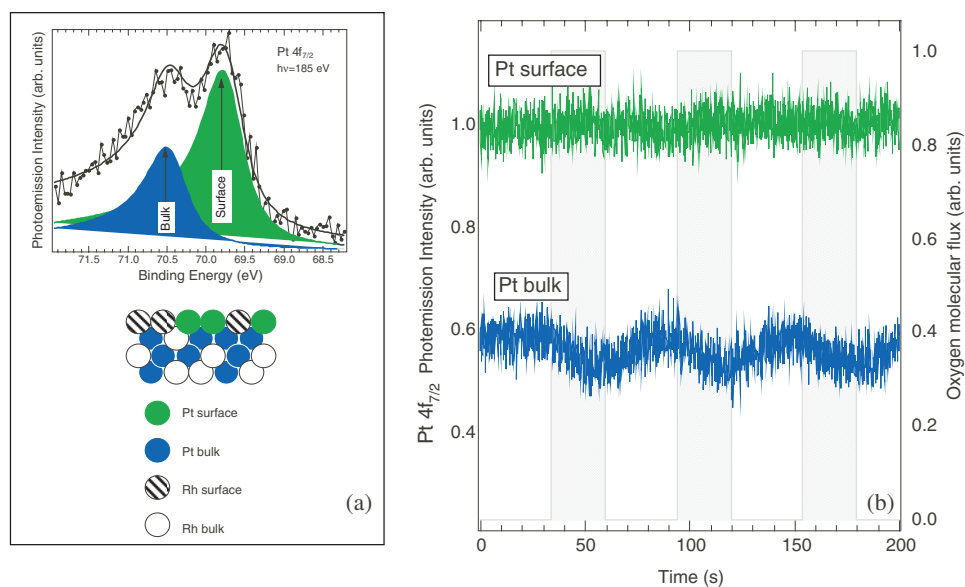


**Figure 9.** (a) A snapshot XPS spectrum, acquired in 100 ms, of Pt  $4f_{7/2}$  from a  $Pt_{50}Rh_{50}(100)$  single-crystal alloy. The surface (binding energy of 70.50 eV, green) and bulk (binding energy of 69.81 eV, blue) components determined from the fit are also shown. (b) Temporal evolution of the bulk and surface Pt population during the reaction with  $H_2$  and  $O_2$ . The ‘ON’ and ‘OFF’ half-periods of the molecular beam effecting the dosing with  $O_2$  are also shown [7].

surface reactions. The recent addition of the molecular beam to the experimental chamber will allow state-selected adsorption studies, i.e. it will be possible to study the dependence of the adsorption mechanisms on the energy and direction of the impinging molecules. Moreover, we plan to perform stroboscopic measurements by chopping the molecular beam. This should allow us to reach data acquisition times shorter than 1 ms.

### Acknowledgments

The results presented in this paper could not have been obtained without the contributions of all the members of the SuperESCA group at the ELETTRA synchrotron radiation facility. Thanks are due to Silvano Lizzit for a critical reading of the manuscript.

### References

- [1] Umbach E, Fuggle J C and Menzel D 1977 *J. Electron Spectrosc. Relat. Phenom.* **10** 15
- [2] Abrami A *et al* 1995 *Rev. Sci. Instrum.* **66** 1618
- [3] Petersen H 1982 *Opt. Commun.* **40** 402
- [4] Jark W 1992 *Rev. Sci. Instrum.* **63** 1241
- [5] Baraldi A and Dhanak V R 1994 *J. Electron Spectrosc. Relat. Phenom.* **67** 211
- [6] Gori L, Tommasini R, Cautero G, Giuressi D, Barnaba M, Accardo A, Carrato S and Paolucci G 1999 *Nucl. Instrum. Methods A* **431** 338
- [7] Baraldi A, Rumiz L, Moretuzzo M, Barnaba M, Comelli G, Lizzit S, Paolucci G, Rosei R, Buatier de Mongeot F and Valbusa U 2001 at press
- [8] Baraldi A, Comelli G, Lizzit S, Cocco D, Paolucci G and Rosei R 1996 *Surf. Sci.* **367** L67
- [9] Dhanak V R, Baraldi A, Comelli G, Paolucci G, Kiskinova M and Rosei R 1993 *Surf. Sci.* **295** 287

- 
- [10] Mårtensson N and Nilsson N 1994 *High Resolution Core-Level Photoelectron Spectroscopy of Surfaces and Adsorbates (Springer Series in Surface Science vol 35)* ed W Eberhardt (Berlin: Springer)
- [11] Joyce J J, Del Giudice M and Weaver J H 1989 *J. Electron Spectrosc. Relat. Phenom.* **49** 31
- [12] Dhanak V R, Comelli G, Cautero G, Paolucci G, Prince K C, Kiskinova M and Rosei R 1992 *Chem. Phys. Lett.* **188** 237
- [13] Comelli G, Baraldi A, Lizzit S, Cocco D, Paolucci G, Rosei R and Kiskinova M 1996 *Chem. Phys. Lett.* **261** 253
- [14] Baraldi A, Lizzit S, Cocco D, Comelli G, Paolucci G, Rosei R and Kiskinova M 1997 *Surf. Sci.* **385** 376
- [15] Root T W, Fisher G B and Schmidt L D 1986 *J. Chem. Phys.* **85** 4679
- [16] Root T W, Fisher G B and Schmidt L D 1986 *J. Chem. Phys.* **85** 4687
- [17] Lizzit S, Baraldi A, Cocco D, Comelli G, Paolucci G, Rosei R and Kiskinova M 1998 *Surf. Sci.* **410** 228
- [18] Baraldi A, Lizzit S and Paolucci G 2000 *Surf. Sci.* **457** L354
- [19] Baraldi A, Lizzit S, Comelli G and Paolucci G 2001 *Phys. Rev. B* **63** 115410
- [20] Cardillo M J 1982 *Annu. Rev. Phys. Chem.* **32** 332
- [21] Baraldi A *et al* 2001 at press